

Periodic structures in integrated optics*

C. Elachi and C. Yeh

Electrical Sciences and Engineering Department, University of California, Los Angeles, California 90024
and

Jet Propulsion Laboratory, California Institute of Technology, Pasadena, California 91109

(Received 11 January 1973; in final form 12 March 1973)

Thin-film dielectric waveguides with a periodic refractive index, a periodic substrate, or periodic surface are studied. The field is determined from Maxwell's equations using Floquet's theorem. The Brillouin diagram and the interaction regions are investigated. The bandwidth and the attenuation coefficients of the interaction regions are given as a function of the optical wavelength. A number of applications in active and passive integrated optics systems are discussed.

I. INTRODUCTION

The recent introduction of the concept of integrated optics¹⁻³ has stimulated a great deal of interest in the design of thin-film miniaturized optical systems. In the last three years, many experiments have been performed in light generation, waveguiding, coupling, deflection, parametric interactions, and others in thin-film structures.¹⁻⁴

Periodic dielectric structures can be used in many integrated optical devices. The periodicity could be generated either by chemical processes, by ion milling, by volume or surface acoustic waves, by electro-optical periodic systems, or by photodimer memories.⁵⁻⁹ Such structures could be used in DFB (distributed feed-back) lasers,^{9,10} integrated optics filter, frequency-selective couplers, and phase-matchable nonlinear interactions.⁸

In this paper we shall study the waveguiding properties of three important types of periodic structures: periodically inhomogeneous thin-film waveguide [Fig. 1(a)], periodically inhomogeneous substrate guide [Fig. 1(b)], and thin-film waveguide with periodic surfaces (periodic thickness) [Fig. 1(c)].

We shall first obtain the general solutions of the wave equation in sinusoidally stratified media. The solutions will then be applied to three specific periodic structure problems as mentioned earlier. Many possible applications of this type of periodic structure to passive and active integrated optics systems will be discussed.

II. SOLUTION OF THE WAVE EQUATION IN PERIODICALLY STRATIFIED DIELECTRIC MEDIA

The source-free wave vector equations in a medium whose permittivity is a function of z , the axial coordinate, are¹¹

$$\nabla \times \nabla \times \mathbf{E} - k_0^2 [\epsilon(z)/\epsilon_0] \mathbf{E} = 0, \quad (1)$$

$$\nabla \times \nabla \times \mathbf{H} - [\nabla \epsilon(z)/\epsilon(z)] \times \nabla \times \mathbf{H} - k_0^2 [\epsilon(z)/\epsilon_0] \mathbf{H} = 0, \quad (2)$$

where $k_0 = \omega(\mu_0\epsilon_0)^{1/2}$, ϵ_0 and μ_0 are, respectively, the free-space permittivity and permeability, \mathbf{E} and \mathbf{H} are, respectively, the electric and magnetic field vectors, a time dependence $\exp(-i\omega t)$ is assumed and suppressed throughout, and $\epsilon(z)$ is the dielectric permittivity of the inhomogeneous medium. Let $\epsilon(z)$ be a periodically varying function of z :

$$\epsilon(z) = \epsilon[1 + \eta f(Kz)],$$

where η and K are known constants and $f(\xi)$ is a periodic

function. The solution of the wave equation consists of an infinite number of space harmonics (Floquet form). For the TE wave, we can write (for propagation in the xz plane)

$$\mathbf{E}^{(TE)} = \mathbf{e}_y \sum_{n=-\infty}^{+\infty} C_n^{TE} \left(\frac{\sin(s_n x)}{\cos(s_n x)} \right) \exp(i\kappa_n z); \quad (3)$$

and for the TM wave,

$$\mathbf{H}^{(TM)} = \mathbf{e}_y \sum_{n=-\infty}^{+\infty} C_n^{TM} \left(\frac{\sin(p_n x)}{\cos(p_n x)} \right) \exp(i\kappa'_n z); \quad (4)$$

where η is an integer, s_n and p_n are separation constants, C_n^{TE} and C_n^{TM} are the amplitudes of the space harmonics, and κ_n and κ'_n are the propagation constants

$$\kappa_n = \kappa + nK,$$

$$\kappa'_n = \kappa' + nK,$$

where κ and κ' may be determined from the dispersion relation and the boundary conditions of various problems that we shall consider.

Replacing \mathbf{E} and \mathbf{H} by their Floquet form in Eqs. (1) and (2), replacing $\epsilon(z)$ by its exponential Fourier series, and equating the terms with the same z dependence, we obtain the following set of infinite equations:

$$(\kappa_n^2 + s_n^2)C_n^{TE} - \frac{k_0^2}{\epsilon_0} \sum_{m=-\infty}^{+\infty} a_{n-m} C_m^{TE} = 0, \quad (5)$$

$$(\kappa_n'^2 + p_n^2)C_n^{TM} - \frac{k_0^2}{\epsilon_0} \sum_{m=-\infty}^{+\infty} L_{nm} C_m^{TM} = 0, \quad (6)$$

$$L_{nm} = a_{n-m} \pm \frac{\epsilon_0 K}{k_0^2} \sum_{l=-\infty}^{+\infty} l a_l a'_{n-l-m},$$

where a_j and a'_j are the Fourier series coefficients of $\epsilon(z)$ and $1/\epsilon(z)$. The solution of the above equations gives the relative amplitudes C_n^{TE}/C_0^{TE} and C_n^{TM}/C_0^{TM} . C_0^{TE} and C_0^{TM} can be determined from the source condition (or the excitation condition).¹² The nontriviality condition gives the dispersion relation.

III. THIN-FILM LONGITUDINALLY INHOMOGENEOUS OPTICAL WAVEGUIDE

In this section we shall consider the problem of the propagation of a transverse electric wave (TE) along a thin-film optical waveguide where the permittivity varies as [Fig. 1(a)]

$$\epsilon(z) = \epsilon_1 [1 + \eta \cos Kz],$$

and where the thickness is $2L$. This waveguide is sub-

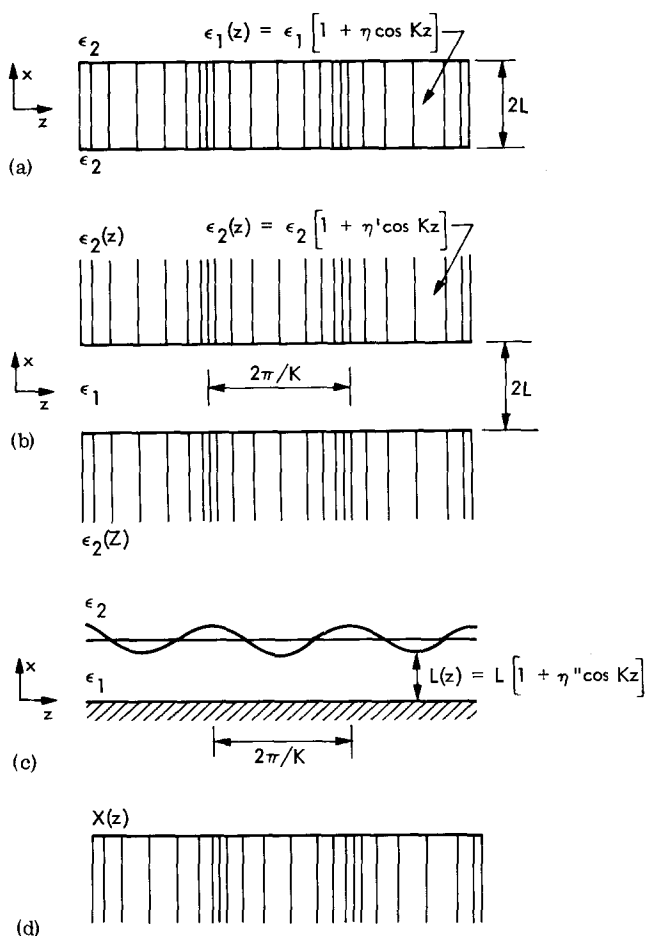


FIG. 1. Geometry of the periodic structures. In (d), $X(z)$ is the surface impedance.

merged in a uniform medium of dielectric constant ϵ_2 with $\epsilon_2 < \epsilon_1$.

Substituting Eq. (3) into Eq. (1) gives the electric field component of the TE wave [$\mathbf{E}(x, z) = E_y(x, z)\mathbf{e}_y$] within the inhomogeneous layer:

$$E_y = \sum_{n=-\infty}^{+\infty} A_n u_n(x) \exp(ik_n z); \quad (7)$$

where $u_n(x) = \cos(s_n x)$ (for even mode) or $\sin(s_n x)$ (for odd mode), and A_n are yet unknown amplitudes of the space harmonics. Since the fields are independent of y , all other components of the electric field are zero. In

the surrounding medium, we have for the guided waves

$$E_y = \sum_{n=-\infty}^{+\infty} A'_n \exp(ik_n z - \delta_n |x|), \quad \text{for } |x| > L, \quad (8)$$

where A'_n are yet unknown amplitudes of the space harmonics and δ_n is the transverse wave number. The magnetic field components may be found from Maxwell's equations.

The boundary conditions at $|x| = L$ demand the continuity of the tangential electric and magnetic field. Hence, we have

$$\begin{aligned} A_n u_n(L) &= A'_n \exp(-\delta_n L), \\ A_n \frac{du_n}{dx} \Big|_{x=L} &= -A'_n \delta_n \exp(-\delta_n L). \end{aligned} \quad (9)$$

Simplifying,

$$\begin{aligned} \delta_n &= s_n \tanh s_n L \quad (\text{even modes}) \\ &= s_n (-\cot s_n L) \quad (\text{odd modes}). \end{aligned} \quad (10)$$

From the wave equation, one has

$$\kappa_n^2 - \delta_n^2 = \mu_0 \epsilon_2 \omega^2 \quad (11)$$

and

$$D_n A_n u_n(x) + A_{n+1} u_{n+1}(x) + A_{n-1} u_{n-1}(x) = 0, \quad (12)$$

where

$$D_n = \frac{2}{\eta} \left(1 - \frac{s_n^2 + \kappa_n^2}{\mu_0 \epsilon_1 \omega^2} \right).$$

To simplify the notation, we did not include the index corresponding to different possible waveguide modes. Equation (12) cannot be satisfied for all x , but as we will only study the interaction regions of identical modes in the limit η small, the $u_n(x)$ will be the same for the two phase-matched space harmonics.

When $\eta = 0$, Eq. (12) gives $\eta D_n = 0$; hence,

$$\kappa_n^2 + s_n^2 = \mu_0 \epsilon_1 \omega^2 \quad (13)$$

and the resulting Brillouin diagram $\omega(\kappa)$ consists of an infinite number of identical curves centered at $\kappa = -nK$. Each curve is identical to the well-known Brillouin curve of a homogeneous dielectric waveguide (Fig. 2). For $\eta = 0$, only the central curve has physical meaning. Since we are mainly interested in the bounded wave, the following condition must be satisfied:

$$\kappa_n^2 > \mu_0 \epsilon_2 \omega^2, \quad (14)$$

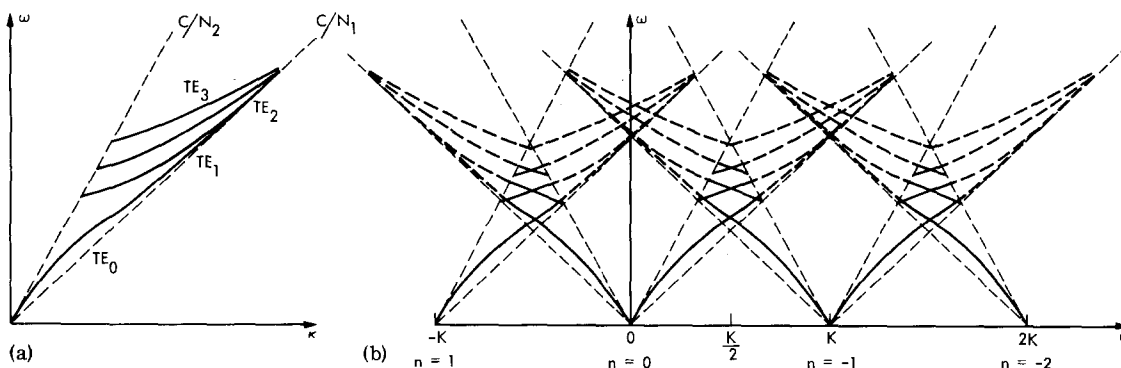


FIG. 2. (a) ω - κ diagram (Brillouin diagram) for a typical dielectric waveguide. (b) ω - κ diagram for a typical periodic dielectric waveguide.

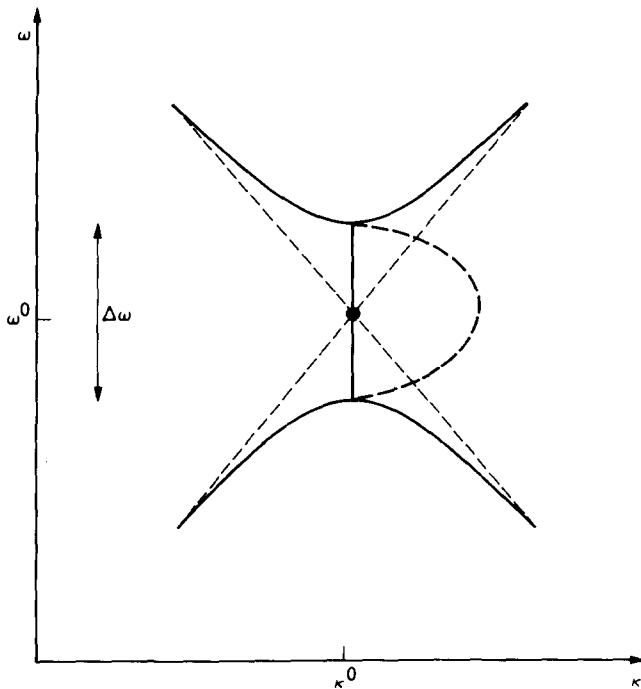


FIG. 3. ω - κ diagram near an interaction region. The solution for κ is complex. The dashed curve is the imaginary part of κ and the solid curve is the real part of κ .

and the corresponding region is shown in Fig. 2. It shows that only successive space harmonics intersect in the bounded region.¹³

For $\eta \neq 0$, strong coupling occurs at the intersection points leading to stop-band interactions (complex κ) between identical modes of successive space harmonics. The behavior of κ near those points requires the solution of the nontriviality condition of the system of Eq. (12). For small values of η , a first-order Taylor series development which takes into account only the two interacting space harmonics can be used to determine the solution in the interaction regions between successive space harmonics.

This paper is confined to the study of stop-band interactions. The codirectional passive interactions are not studied because, in most practical cases, the refractive indices of the film and the substrate are not very different from each other, and these interactions occur in the radiation region of the Brillouin diagram.

In order that interactions between harmonics of the m th mode may occur, the following condition must be satisfied:

$$\frac{K}{2} > \kappa_{\text{cutoff}} \text{ (of the } m\text{th mode)} = \frac{N_2}{(N_1^2 - N_2^2)^{1/2}} \frac{m\pi}{2L}.$$

This implies that

$$\Lambda = \frac{2\pi}{K} < \frac{2L}{m} \left(\frac{N_1^2}{N_2^2} - 1 \right)^{1/2}, \quad (15)$$

where $N_1^2 = \epsilon_1/\epsilon_0$ and $N_2^2 = \epsilon_2/\epsilon_0$.

Consider now the interaction point ($\omega^0, \kappa^0 = \frac{1}{2}K$) between the space harmonics $n=0$ and $n=-1$. Near that point we can write

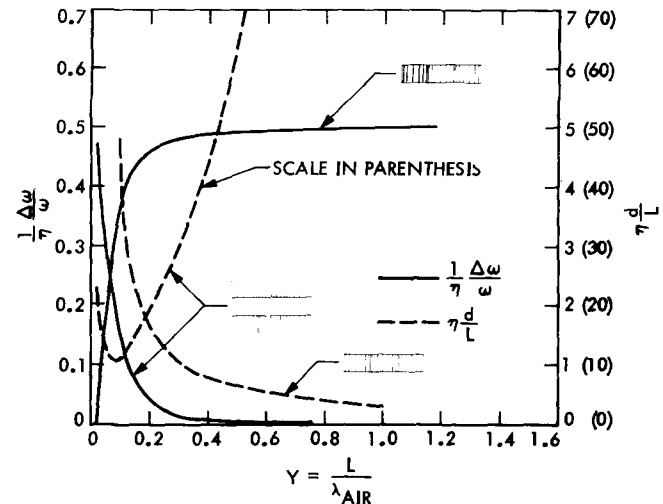


FIG. 4. Plots of the relative width $(1/\eta)\Delta\omega/\omega$ and attenuation factor $\eta d/L$ for the first interaction region of the main even mode as a function of L/λ_0 . λ_0 is wavelength in vacuum. The cases of a periodic waveguide and a periodic substrate are plotted. The waveguide index is $N_1=2$ and the substrate index is $N_2=1.5$.

$$\kappa = \kappa^0(1 + \eta g) \quad \text{and} \quad \omega = \omega^0(1 + \eta f),$$

and $u_0 \approx u_{-1}$. The system of Eqs. (12) reduces to

$$\begin{cases} D_0 A_0 + A_{-1} = 0 \\ D_{-1} A_{-1} + A_0 = 0 \end{cases} \Rightarrow D_0 D_{-1} = 1. \quad (16)$$

Applying the Taylor series development to Eqs. (10), (11), and (16), we get

$$\alpha^2 f^2 - g^2 = \beta^2, \quad (17)$$

where

$$\alpha = \left(\frac{2\omega^0}{Kc} \right)^2 \left(\frac{N_2^2 + qN_1^2}{1+q} \right),$$

$$\beta = \left(\frac{N_1\omega^0}{Kc} \right)^2 \left(\frac{q}{1+q} \right),$$

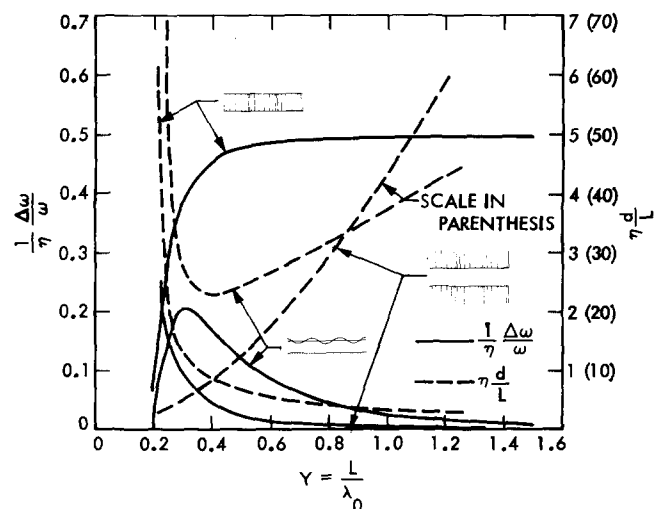


FIG. 5. Plots of the relative width $(1/\eta)\Delta\omega/\omega$ and attenuation factor $\eta d/L$ for the first interaction region of the first odd mode as a function of L/λ_0 . λ_0 is wavelength in vacuum. The cases of a periodic waveguide, periodic surface, and a periodic substrate are plotted. The waveguide index is $N_1=2$ and the substrate index is $N_2=1.5$.

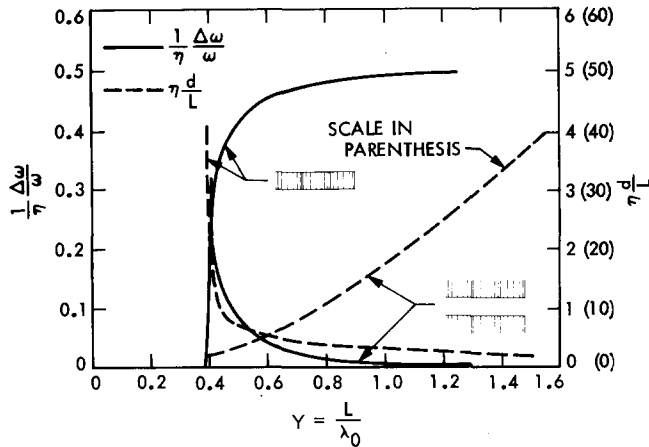


FIG. 6. Plots of the relative width $(1/\eta)\Delta\omega/\omega$ and attenuation factor $\eta d/L$ for the first interaction region of the second even mode as a function of L/λ_0 . λ_0 is wavelength in vacuum. The cases of a periodic waveguide and a periodic substrate are plotted. The waveguide index is $N_1=2$ and the substrate index is $N_2=1.5$.

$$q = \left(\frac{\delta^0}{s^0} \right)^2 \left(1 \pm \frac{s^0 L}{\sin s^0 L \cos s^0 L} \right),$$

where the \pm sign corresponds to the even(+) and odd(-) modes, and the values of δ^0 and s^0 correspond to ω^0 and κ^0 . Equation (16) corresponds to a hyperbola for $|f| \geq \beta/\alpha$ and an ellipse (g imaginary) for $|f| < \beta/\alpha$, as sketched in Fig. 3. The two characteristic parameters of interest are the relative bandwidth of the interaction $\Delta\omega/\omega = 2\eta\beta/\alpha$, and the maximum of imaginary (κ) $= \eta K\beta/2$ and its inverse d . In Figs. 4–6 we plot these two parameters as a function of L/λ , where λ corresponds to the free-space wavelength for the first two even modes and the first odd mode. In all these cases, the interaction is most efficient ($d/L \rightarrow 0$) when the energy of the wave is mostly confined within the waveguide (i.e., $L/\lambda \rightarrow \infty$).

IV. HOMOGENEOUS THIN-FILM WAVEGUIDE SURROUNDED BY A LONGITUDINALLY PERIODIC MEDIUM

Let us now treat the problem of a TE wave propagating along a homogeneous thin film immersed in an inhomogeneous medium whose dielectric constant is given by

$$\epsilon_2(z) = \epsilon_2(1 + \eta' \cos Kz).$$

The dielectric constant of the film is ϵ_1 [see Fig. 1(b)]. This problem may be solved in a manner similar to the previous case. The corresponding systems of equations to be solved are Eq. (10) and

$$s_n^2 + \kappa_n^2 = \mu_0 \epsilon_1 \omega^2, \quad (18)$$

$$D'_n A'_n \exp(-\delta_n x) + A'_{n+1} \exp(-\delta_{n+1} x) + A'_{n-1} \exp(-\delta_{n-1} x) = 0, \quad (19)$$

where

$$D'_n = \frac{2}{\eta'} \left(1 - \frac{\kappa_n^2 - \delta_n^2}{\mu_0 \epsilon_2 \omega^2} \right).$$

The limitations on the solution of Eq. (19) are the same as for Eq. (12). The Brillouin diagram is the same as in Fig. 2 and the solution in the interaction region for

small η' is

$$\alpha^2 f^2 - g^2 = \beta'^2,$$

where

$$\beta' = (N_2 \omega^0 / Kc)^2 (1 + q)^{-1}.$$

The corresponding characteristic parameters are given in Table I and plotted in Figs. 4–6. Unlike the previous case, we note that mode interaction occurs most efficiently near the cutoff where most of the energy is in the substrate. The mode interaction characteristics for these two structures are equivalent if η and η' satisfy the following relation:

$$\eta\beta = \eta'\beta' \Rightarrow \eta/\eta' = \beta'/\beta.$$

This ratio is plotted in Fig. 7.

V. OPTICAL GUIDE WITH SINUSOIDALLY VARYING SURFACE

The third problem we shall consider is the case of a TE wave propagating along an optical thin-film guide whose surface is a sinusoidal function of the longitudinal coordinate [Fig. 1(c)]; i.e.,

$$L(z) = L[1 + \eta'' \cos Kz].$$

The substrate is assumed to be a perfect conductor and the upper half-space has a dielectric constant $\epsilon_2 < \epsilon_1$. We assume $\eta'' KL \ll 1$, so that the Rayleigh assumption¹⁴ for scattering from periodic surfaces is valid.

Owing to the boundary periodicity, the field is the sum of an infinite number of space harmonics (Floquet's theorem). Therefore, the field expression can be written as follows (we are mainly interested in the bounded wave):

$$E = \sum_{n=-\infty}^{+\infty} A_n \sin(s_n x) \exp(ik_n z), \quad \text{for } 0 < x \leq L(z) \\ = \sum_{n=-\infty}^{+\infty} A'_n \exp(-\delta_n |x| + ik_n z), \quad \text{for } x \geq L(z),$$

where A_n and A'_n are the amplitudes of the space harmonics. The above expressions satisfy the boundary

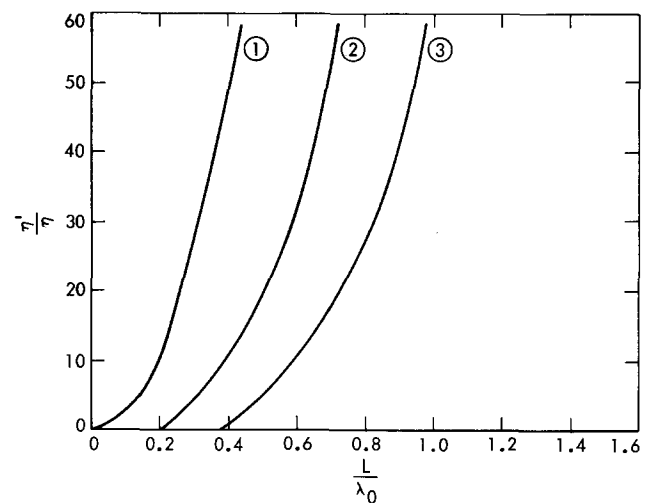


FIG. 7. Equivalence ratio η'/η between the periodic substrate and periodic waveguide configuration. Curve 1 corresponds to the basic even mode. Curve 2 corresponds to the first odd mode. Curve 3 corresponds to the second even mode.

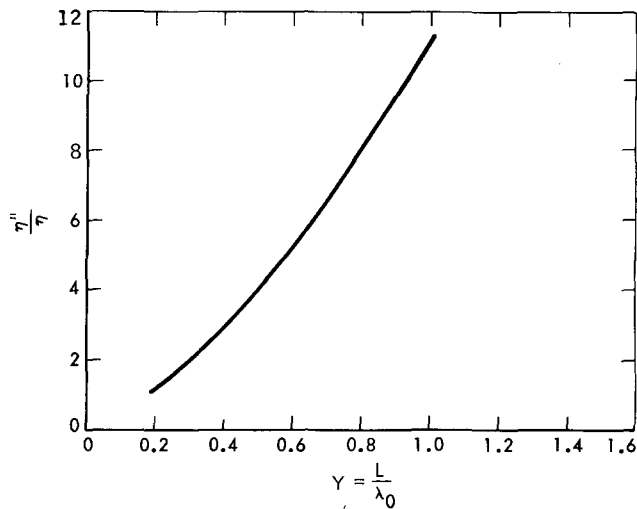


FIG. 8. Equivalence ratio η''/η between the periodic thickness and periodic waveguide index configuration for the first odd mode.

condition at $x=0$. From Maxwell's equations we may obtain the following relations:

$$\kappa_n^2 + s_n^2 = \mu_0 \epsilon_1 \omega^2, \quad (20)$$

$$\kappa_n^2 - \delta_n^2 = \mu_0 \epsilon_2 \omega^2. \quad (21)$$

The boundary conditions at $x=L(z)=L(1+\eta''\cos Kz)$ are (i) tangential \mathbf{E} must be continuous; and (ii)

$$(\mathbf{H} - \mathbf{H}') \times \mathbf{e} = 0, \quad (22)$$

where \mathbf{e} is a unit vector normal to the surface $= (\mathbf{e}_x + \eta''KL \sin Kz \mathbf{e}_z) / (1 + \eta''^2 K^2 L^2 \sin^2 Kz)^{1/2}$ and \mathbf{H} and \mathbf{H}' are the magnetic field on both sides of the boundary.

From condition (i) and the field expression we get, after applying a first-order Taylor series development ($\eta''KL \ll 1$),

$$\begin{aligned} \sum_n A_n (\sin s_n L + \eta'' s_n L \cos Kz \cos s_n L) \exp(ik_n z) \\ = \sum_n A'_n (1 - \eta'' \delta_n L \cos Kz) \exp(ik_n z). \end{aligned}$$

Writing $\cos Kz$ in an exponential form and equating the terms with the same longitudinal wave vector, we get

$$\begin{aligned} (a_n/s_n) \tan s_n L + \frac{1}{2} \eta'' L (a_{n+1} + a_{n-1}) - (b_n/\delta_n) \\ + \frac{1}{2} \eta'' L (b_{n+1} + b_{n-1}) = 0, \end{aligned} \quad (23)$$

where $a_n = s_n A_n \cos(s_n L)$ and $b_n = \delta_n A'_n \exp(-\delta_n L)$. Similarly, from Eq. (22) we find

$$\begin{aligned} a_n - \frac{1}{2} \eta'' L (C_{n+1} a_{n+1} + C_{n-1} a_{n-1}) + b_n \\ + \frac{1}{2} \eta'' L (B_{n+1} b_{n+1} + B_{n-1} b_{n-1}) = 0, \end{aligned} \quad (24)$$

where

$$C_n = [(K\kappa_n + s_n^2)/s_n] \tan s_n L, \quad B_n = (K\kappa_n - \delta_n^2)/\delta_n.$$

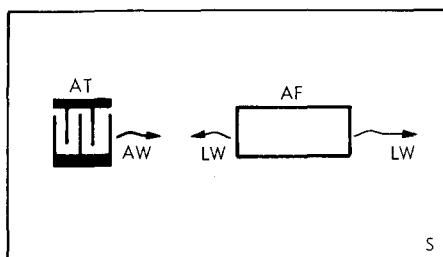
The infinite systems of Eqs. (23) and (24) can be written in a matrix form:

$$||M|| \cdot |a| = ||N|| \cdot |b|,$$

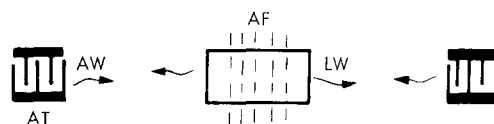
$$||P|| \cdot |a| = ||Q|| \cdot |b|,$$

or

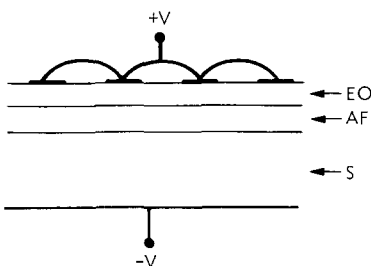
$$(|M| - |N| \cdot |Q|^{-1} \cdot |P|) \cdot |a| = 0, \quad (25)$$



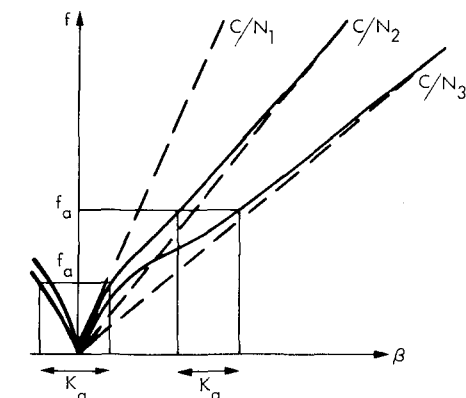
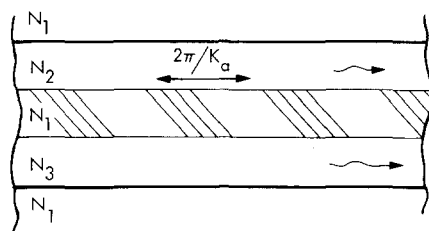
(a)



(b)



(c)



(d)

FIG. 9. Some optical systems using periodic structures; (a) DFB laser using a propagating acoustic wave; (b) DFB pulsing laser using a stationary acoustic wave; (c) DFB laser using an electro-optic periodic structure; (d) frequency-selective coupler with the corresponding Brillouin diagram. AT—acoustic transducer; AF—amplifying film; AW—acoustic wave; LW—light wave; EO—electro-optic film, S—substrate.

TABLE I. Characteristic parameters with $Y = \omega L / 2\pi c$.

Structure	$\frac{1}{\eta} \frac{\Delta\omega}{\omega}$	$\frac{\eta d}{L}$	$\frac{\Delta\omega}{\omega} \frac{d}{L}$
periodic waveguide index	$\frac{qN_1^2}{2(N_2^2 + qN_1^2)}$	$\frac{L}{\Lambda} \frac{1+q}{q} \frac{1}{\pi N_2^2 Y^2}$	$\frac{L}{2\Lambda} \frac{1+q}{N_2^2 + qN_1^2} \frac{1}{\pi Y^2}$
periodic substrate index	$\frac{N_1^2}{2(N_2^2 + qN_1^2)}$	$\frac{L}{\Lambda} (1+q) \frac{1}{\pi N_2^2 Y^2}$	same as above
periodic waveguide thickness	$(\delta^0 L)^2 \frac{N_1^2 - N_2^2}{N_2^2 + qN_1^2}$	$\frac{K}{\delta^0} \frac{1+q}{(N_1^2 - N_2^2)(2\pi Y)^2}$	same as above

where the elements of the matrices $\|M\|$, $\|N\|$, $\|P\|$, and $\|Q\|$ can be easily determined from Eqs. (23) and (24). The nontriviality condition of Eq. (25), with Eqs. (20) and (21), gives the dispersion relation $\kappa(\omega)$ and the relative amplitudes a_n/a_0 and b_n/a_0 .

For $\eta'' = 0$, Eqs. (23) and (24) reduce to

$$(a_n/s_n) \tan s_n L = b_n/\delta_n,$$

$$a_n = -b_n,$$

or

$$\delta_n = -s_n \cot s_n L. \quad (26)$$

The corresponding Brillouin diagram is the same as for the previous cases (odd modes only).

For small $\eta'' \neq 0$, a first-order Taylor series development gives

$$\alpha^2 f^2 - g^2 = \beta''^2,$$

where

$$\beta'' = \frac{2\delta^0 L}{1+q} (N_1^2 - N_2^2) \left(\frac{\omega^0}{Kc} \right)^2.$$

The two characteristic parameters $\Delta\omega/\omega$ and d/L are given in Table I and plotted in Fig. 6 for the first mode with $N_2 = 1.5$ and $N_1 = 2$. We see that for $\omega \rightarrow \infty$ ($L/\lambda \rightarrow \infty$), the periodicity has little effect ($d/L \rightarrow \infty$, $\Delta\omega/\omega \rightarrow 0$) because the wave energy is mostly confined inside the waveguide and is not near the boundary. The boundary periodicity has also little effect on the propagating waves in the limit $\omega \rightarrow \omega_{\text{cutoff}}$ when most of the energy is in the substrate. The boundary perturbation is most effective for $L/\lambda \approx 0.35$, where $d/L = 2.3/\eta$ and $\Delta\omega/\omega = 0.2\eta$.

In Fig. 8 we plotted the equivalence ratio η''/η between the surface periodic case and the inside index periodic case.

Another interesting structure which can be treated in a similar way is shown in Fig. 1(d)—the dielectric waveguide which has a periodic boundary impedance

$$Z = iX_0[1 + \eta \cos Kz].$$

Such an impedance can be generated by using a grooved substrate. This impedance can be controllable (slightly), for matching purposes, by filling the substrate grooves with an electro-optic material whose index (and, therefore, the effective groove depth) can be controlled by an applied electric voltage.

VI. DISCUSSIONS AND POSSIBLE APPLICATIONS

Periodic structures can be of two types: (i) permanent, where the periodicity in the refractive index, gain coefficient (in the case of an active medium), and boundary of the optical medium is permanent (chemical, doping, ion implementation, or others). This type of structure was used in DFB lasers^{10,15} and in couplers. (ii) Non-permanent or dynamically controllable, where the periodicity can be easily written and erased (photodimer memories,⁶ electro-optical periodic structures), or is dynamically controllable (beam interference,⁷ surface or bulk acoustic waves). We shall now discuss the application of some of these structures in active and passive integrated optics systems.

Periodic structures in amplifying films are used in DFB lasers.^{10,15,16} Kogelnik and Shank¹⁰ showed that very small changes (10^{-4} – 10^{-5}) in the refractive index of the guiding film are sufficient to generate oscillation in a DFB laser. Using the results of Sec. V and Fig. 8, we see that this is equivalent to boundary rippling of the order of 10 – 20 Å depending on the guide parameters. This surface perturbation could be obtained by a surface acoustic wave [Fig. 9(a)]. The lasing wavelength of the DFB laser is given by the Bragg condition (neglecting the acoustic wave motion):

$$\lambda_0 = 2N_1\Lambda/m,$$

where m is an integer. Therefore, the acoustic frequency falls in the range of few GHz. This domain of the acoustic spectrum is of great interest in integrated acoustics and it is presently possible to fabricate such surface-wave devices for operating frequencies up to 3 GHz.¹⁷ In Fig. 9(b), a second acoustic transducer, at 180° from the first one, would generate a standing acoustic wave leading to a DFB laser pulsing at twice the acoustic frequency. The lasing frequency can be tuned by changing the acoustic frequency.

The electro-optic effect can also be used in thin-film structures.^{1,18} If a spatial periodic electric voltage is applied to an electro-optic material, the resulting periodicity generates the DFB effect. The electro-optic material can be used as a substrate or as a matrix for the lasing material [Fig. 9(c)]. Index change of the order of 10^{-4} can be easily achieved with only a few volts. Periodic structures using the electro-optic effect have also been used for wave modulation.¹⁹

In passive systems, periodic structures can be used for distributed selective coupling between two closely spaced waveguides.²⁰ They have already been used for the coupling of a free wave to a waveguide. Let us now consider the system shown in Fig. 9(d). It can be easily seen that there is no evanescent coupling for the fundamental mode at all frequencies since, for a given f , β is not the same in both guides, and the periodic structure would only couple a signal of frequency f_c , even if the waveguides may carry a large number of signals with different frequencies. To obtain optimum coupling, the parameters must be adequately chosen. Such a system can be designed to yield selective coupling at two or more specific frequencies, if we make adequate use of the different modes of the waveguides and the guide

dimensions. If the periodic structure is of the dynamic type, the frequencies can be varied. The frequency-selective coupler can be used as the basic unit of an optical multiplexer to select specific channels from a large number of communication channels in a thin-film guide.

Another application is the use of the periodic structures as integrated optical filters. For an $0.8\text{-}\mu$ film with a surface rippling of 40 \AA and an optical wavelength of $\lambda_0 = 0.8\text{ }\mu$, the attenuation factor could reach 14 dB/mm (power).

In conclusion, we note that periodic structures have characteristics which can be used in many active and passive integrated-optics systems. The stop-band pass-band property can be used to design integrated optics filters. Attenuations of the order of tens of dB/mm can be easily obtained. The feedback property of periodic structures can be used in active systems to design DFB lasers. Different configurations can be used: index periodicity in the film, index periodicity of the substrate, or film-thickness periodicity. The presence of space harmonics with different phase velocities can also be used for phase-matched nonlinear interactions.

*Partly supported by the Naval Electronics Laboratory Center and partly supported by NASA under Contract No. NAS7-100.

¹P. K. Tien, Appl. Opt. **10**, 2395 (1971).

²S. E. Miller, Bell Syst. Tech. J. **48**, 2059 (1969).

³R. Shubert and J. H. Harris, IEEE Trans. Microwave Theory Tech. **16**, 1048 (1968).

⁴J. L. Altman, *Microwave Circuits* (Nostrand, Princeton, N.J., 1964).

⁵P. K. Tien, Appl. Opt. **11**, 205 (1972).

⁶R. L. Fork, K. R. German, and E. A. Chandross, Appl. Phys. Lett. **20**, 139 (1972).

⁷R. V. Pole, S. E. Miller, J. H. Harris, and P. K. Tien, Appl. Opt. **11**, 1675 (1972).

⁸S. Somekh and A. Yariv, Appl. Phys. Lett. **21**, 140 (1972).

⁹J. E. Bjorkholm and C. V. Shank, Appl. Phys. Lett. **20**, 3061 (1972).

¹⁰H. Kogelnik and C. V. Shank, J. Appl. Phys. **43**, 2327 (1972).

¹¹C. Yeh, K. F. Casey, and Z. A. Kaprielian, IEEE Trans. Microwave Theory Tech. **13**, 297 (1965).

¹²C. Elachi, IEEE Trans. Antennas Propag. **20**, 280 (1972).

¹³E. S. Cossedy, Proc. IEEE **112**, 269 (1965).

¹⁴Lord Rayleigh, *The Theory of Sound* (Dover, New York, 1945), Vol. II.

¹⁵D. P. Schinke, R. G. Smith, E. G. Spencer, and M. F. Galvin, Appl. Phys. Lett. **21**, 494 (1972).

¹⁶K. O. Hill and A. Watanabe, Opt. Commun. **5**, 389 (1972).

¹⁷R. M. White, Proc. IEEE **58**, 1238 (1970).

¹⁸D. J. Channin, Appl. Phys. Lett. **19**, 128 (1971).

¹⁹D. P. Gia Russo and J. H. Harris, Appl. Opt. **12**, 2786 (1971).

²⁰C. Elachi and C. Yeh, Optics Comm. (to be published).